PROCEEDINGS, TOUGH Symposium 2003
Lawrence Berkeley National Laboratory, Berkeley, California, May 12–14, 2003

ESTIMATING FLOW PARAMETERS USING GROUND-PENETRATING RADAR AND HYDROLOGICAL DATA DURING TRANSIENT FLOW IN THE VADOSE ZONE

Michael Kowalsky[1], Stefan Finsterle[2], and Yoram Rubin[1]

[1]Dept. of Civil and Environmental Engineering, University of California, Berkeley
Berkeley, CA, 94720, USA
e-mail: MBKowalsky@lbl.gov

[2]Earth Sciences Division, Lawrence Berkeley National Laboratory
Berkeley, CA, 94720, USA

ABSTRACT

Methods for determining the parameters necessary for modeling fluid flow and contaminant transport in the shallow subsurface are in great demand. Soil properties such as permeability, porosity, and water retention are typically estimated through the inversion of hydrological data (e.g., measurements of capillary pressure and water saturation). However, ill-posedness and non-uniqueness commonly arise in such inverse problems making their solutions elusive. Incorporating additional types of data, such as from geophysical methods, may greatly improve the success of inverse modeling. In particular, ground-penetrating radar (GPR) has proven sensitive to subsurface fluid flow processes. In the present work, an inverse technique is presented in which permeability distributions are generated conditional to time-lapsed GPR measurements and hydrological data during a transient flow experiment. Specifically, a modified pilot point framework has been implemented in iTOUGH2 allowing for the generation of permeability distributions that preserve point measurements and spatial correlation patterns while reproducing geophysical and hydrological measurements. Through a numerical example, we examine the performance of this method and the benefit of including GPR data while inverting for fluid flow parameters in the vadose zone. Our hypothesis is that within the inversion framework that we describe, our predictive ability greatly improves with the addition of transient hydrological measurements and geophysical measurements (GPR-derived estimates of water saturation, in particular).

INTRODUCTION

Predicting how quickly a spilled contaminant will migrate through the vadose zone and into an aquifer, or predicting water availability for crops at root zones, for example, depends on soil properties such as permeability, porosity, and water retention. Techniques are available for measuring point values of these fluid flow parameters directly in the field or for soil cores in the laboratory. However, fluid flow parameters are commonly heterogeneous, and uncertainty in their spatial distributions makes it difficult to model fluid flow and contaminant transport from point measurements alone. Furthermore, point measurements are commonly limited due to their collection being expensive, time consuming, and invasive (with the potential for creating preferential flow paths). Techniques allowing for the inference of flow parameter distributions are, therefore, in high demand.

In some cases, when spatial statistics at a given site are known, conditional simulation techniques may be used to generate parameter fields in which point measurements and spatial correlation patterns are preserved. However, fields generated with such techniques do not, in general, accurately predict flow. Parameter inversion techniques are typically required for this purpose.

The development of inverse techniques has allowed for the estimation of flow parameters given both point measurements and hydrological data. While substantial progress has been made in accounting for multi-dimensional spatially heterogeneous flow properties in the saturated zone, inverse methods for the vadose zone are less common and have been mostly concerned with one-dimensional cases, usually uniform or layered soil columns (e.g., Kool et al., 1985; Mishra and Parker, 1989; Simunek and van Genuchten, 1996; Zijlstra and Dane, 1996; Hollenbeck et al., 1998; Zhou et al., 2001). This is in large part due to the difficulty in overcoming ill-posedness and non-uniqueness inherent to such problems (see Carrera and Neuman (1986) and Russo et al. (1991)). One way to make inverse problems more amenable to solution is by including additional types of data. Incorporating geophysical measurements, in particular, into inverse techniques for the vadose zone is a promising area of research (e.g., Hubbard et al., 1997; Binley et al., 2002; Yeh et al., 2002), though still in its infancy.

Generally stated, the inverse problem may be defined as estimating a set of relevant flow parameters given: 1) point measurements of the flow parameters, 2) some hydrological measurements collected during a

flow experiment, along with 3) any other (possibly transient) measurements which are sensitive to flow processes, including geophysical measurements. A solution to this inverse problem is the parameter distribution for which the simulated and measured observational data match (assuming that adequate models exist for simulating each data type), and which preserves parameter measurements.

In the present study, we assume that the absolute permeability is the only non-uniform and unknown flow parameter, and that it is a randomly varying field characterized by known correlation patterns. Through inversion, we attempt to approximate the permeability field using various combinations of measurements including: point measurements of log permeability; water saturation in the boreholes (attainable by methods such as neutron probe logging); and horizontally averaged water saturation values (attainable from zero-offset profile GPR measurements). Additional types of data including capillary pressure and flux measurements can also be easily included in the method we describe.

PROBLEM STATEMENT

For the current study, observational data are generated for a true log permeability model to obtain the measurement vector $\mathbf{z}_{meas} = [\mathbf{z}^{sat}_{meas}, \mathbf{z}^{GPR}_{meas}]$, where $\mathbf{z}^{sat}_{meas}$ and $\mathbf{z}^{GPR}_{meas}$ are the borehole saturation and GPR measurements (both collected in different locations for numerous times), respectively. The measurement/estimation error vector **v** is defined as the difference between the true and measured observation data. A vector of unknown log permeability values is given by **a**, which, after being mapped to the entire flow domain, allows for the simulation of observational data $\mathbf{z}_{sim} = [\mathbf{z}^{sat}_{sim}, \mathbf{z}^{GPR}_{sim}]$, where the subsets of borehole saturation and GPR data types are similarly denoted as for $\mathbf{z}_{meas}$.

Both **a** and **v** are assumed to be independent Gaussian distributions with known covariance matrices C_a and C_v, respectively. Therefore, the estimation problem is of the form of a Gaussian maximum a posteriori formulation (e.g., McLaughlin and Townley, 1996), where the objective function (OF) is given by

$$OF(\mathbf{a}) = [\mathbf{z}_{meas} - \mathbf{z}_{sim}]^T \mathbf{C}_v^{-1} [\mathbf{z}_{meas} - \mathbf{z}_{sim}] + [\mathbf{a} - \bar{\mathbf{a}}]^T \mathbf{C}_a^{-1} [\mathbf{a} - \bar{\mathbf{a}}] \quad (1)$$

where $\bar{\mathbf{a}}$ is the prior estimate of **a**. The first term in (1) represents the mismatch between measured and simulated observations for an estimated **a**, and the second term represents the mismatch between **a** and its prior values. Finding a set of parameters **a** that minimizes (1) defines the inverse problem for the present study.

METHODOLOGY

A means for mapping the discrete values of **a** to the entire flow domain is available through sequential simulation. Estimation of **a** given some measurements is then made possible through inversion with concepts taken from the pilot point method. An overview of the pilot point method is given next, followed by a description of our implementation of the method, and a brief description of the optimization technique employed.

Pilot Point Framework

The pilot point method was originally developed in work such as Marsily (1984) and Certes and Marsily (1991). The essence of the method lies in generating a fluid flow parameter field that honors parameter measurements, and then modifying it in select locations to obtain a better match between measured and simulated observational data, while preserving the known spatial correlation pattern. The set of points that parameterizes the field are called pilot points, and they are estimated through inversion. Application of the method, including how the pilot point locations are chosen, which observational data are used, and details regarding the objective function (e.g., weighting of parameters, observational data, and prior information) differ greatly among previous implementations of the method.

While some of the perceived benefit of early work on the pilot point method derived from its flexibility in choosing pilot point locations, later innovative work involved finding systematic and efficient approaches for positioning pilot points. RamaRao et al. (1995) proposed a method for adding pilot points sequentially, after finding their optimal locations with adjoint sensitivity analyses. Some concerns were later raised regarding the addition of pilot points in this way (Cooley, 2000). In an alternate implementation given by Gomez-Hernandez et al. (1997), pilot points were placed on a pseudo-regular grid and called master points, and inversion for their values was performed simultaneously. They found the optimal master point spacing to be on the order of 2 to 3 points per correlation length.

The pilot point framework is well suited for inclusion of different data types under varied flow conditions. Much of the work mentioned above involved horizontal flow in the saturated zone, where the parameter of interest was the log transmissivity (or the hydraulic conductivity), and observational data included steady-state and transient piezometric measurements. Wen et al. (2002) extended the method of Gomez-Hernandez et al. (1997) to include transient tracer data, and found that that combination

of (noise-free) piezometric head and tracer data improved their ability to predict transport.

In previous work, prior information for pilot points was most often implemented through parameter constraints (i.e., pilot points were allowed to vary freely within strict bounds around the initial values or the kriging estimates (e.g., Certes and Marsily, 1991; La Venua and Pickens, 1992; Hernandez et al., 1997). This is equivalent to minimizing (1) without the second term, and with the error covariance matrix C_v being represented by some relative weighting parameter—though it was often assumed that there was zero measurement/estimation error. The inclusion of prior pilot point information using a "Gaussian regularization term" was suggested as a potential improvement to the method (McLaughlin and Townly, 1996).

Proposed Implementation

In the present work, we consider the case of a vadose zone model in which absolute permeability is an unknown random function, and the remaining flow parameters (e.g., porosity and the parameters describing the capillary pressure function) are considered known and constant. We also assume that the possibly anisotropic correlation function (or semi-variogram) describing the permeability distribution is known (e.g., from an outcrop study). If available, permeability measurements are assumed to be from a support scale equal to that of the grid blocks at which flow is modeled and their error distributions known. In addition, the measurement error distributions are Gaussian with zero mean and known variance.

The objective function we use in this work is equivalent to (1), where the diagonal elements of the pilot point covariance matrix are given by the kriging variance values, and the prior values of the pilot points are taken to be the kriging estimates. If no measurements are available, then the kriging estimates of the prior and the variance values equal the population mean and variance, respectively (i.e., as prior values become more accurate, more weight is given to them).

Since the goal of the method is to predict flow phenomena (rather than obtain a smooth model that represents an average of all possible models), implementation requires multiple inversions with different random field realizations (each with a different seed number). Each of the resulting models is plausible and equally likely given the available data. For increasingly well-designed problems, fewer realizations are required.

For a given realization, a parameter field is generated, and the set of parameters (pilot points), whose locations are defined prior to inversion are estimated simultaneously through inversion. (Note that although there are similarities with this implementation to the method of Gomez-Hernandez et al. (1997), we will refer to the unknowns as pilot points rather than master points). Inversion involves perturbing values at these points, re-generating the parameter field using sequential simulation (in essence propagating the perturbations throughout the parameter field), simulating flow and GPR with the perturbed field, and then evaluating the objective function. The final model is that for which measured and simulated observational data match best.

Implementation details

The method we propose here has recently been implemented in iTOUGH2 (Finsterle, 1999), a code that provides inverse modeling capabilities to the TOUGH2 flow simulator (Pruess, 1999). An outline of the steps in the procedure is as follows:

1) Measurements are collected in a field test (or synthetic data are generated for synthetic study).
2) The number and locations of pilot points is defined.
3) For a given realization (random field seed number), a permeability field **a** is generated. This field is modified in steps 5-6.
4) Simulated measurements $\mathbf{z}_{sim}$ are generated, and used to calculate the initial value of the objective function.
5) Pilot point values are perturbed via an optimization algorithm (described in the next section), and a new field (with the same seed number) is generated using the newly perturbed values. The pilot points are treated as data points in the sequential simulation such that perturbation of a pilot point value is propagated throughout the region near that point, the extent of influence depending on the correlation range of the model.
6) Simulated measurements $\mathbf{z}_{sim}$ are generated with the perturbed field obtained from (5), and used to calculate the new value of the objective function.
7) Steps 5 – 6 are repeated until the solution is found.

Optimization algorithm

The success of any inversion depends on the careful choice and implementation of optimization algorithm. Parameter inversion methods are most commonly performed using gradient based methods (e.g., the Levenberg-Marquardt technique). But, because of the complex nature of inverse problems in the unsaturated zone, the use of non-gradient methods for optimization problems in the unsaturated zone has also been suggested (Pan and Wu, 1998). While usually less efficient than gradient-based methods, non-gradient methods such as Simulated Annealing and Downhill Simplex are robust, less

sensitive to initial conditions, and require no assumptions to be made about the objective function such as it being quadratic or smooth (Pan and Wu, 1998).

For the example shown next, we found the application of gradient-based methods to be unstable. However, inversion using the Downhill Simplex method was found to work well. Two consecutive iterations were performed for each realization to help ensure identification of the global minimum. Details of the Downhill Simplex method and its implementation are not given here but have been well documented elsewhere (e.g., Nelder and Mead, 1965; Press, et al., 1992).

NUMERICAL EXAMPLE

Ponding Experiment

Here we consider a two-dimensional vadose zone model extending 3 meters deep and 4 meters in the horizontal direction with 10 cm nodal spacing in the vertical and horizontal directions. The saturation values of the upper boundary of the model are allowed to vary during an infiltration test, but are considered to be known. To represent the water table, saturation values along the lower boundary of the model are kept fully saturated. The vertical sides of the model are modeled as no-flow boundaries. See Fig. 1 for a schematic of the model.

The soil properties of the model (i.e., the hydraulic conductivity and capillary pressure functions), are described by a commonly used parametric formulation (van Genuchten, 1980). All of the parameters characterizing the soil properties are constant except for the absolute permeability, which is a randomly varying field. Specifically, a log permeability field was generated using sequential Gaussian simulation (SGSIM) (Deutsch and Journel, 1992). This field, shown in Fig. 2a, was generated using an anisotropic Gaussian correlation function with effective horizontal and vertical ranges of 1.5 m, and 0.75 m, respectively, and with a variance of 0.5 m^2, and a nugget value of 0.01 m^2.

To simulate a ponding infiltration experiment, fully saturated conditions were imposed at the surface over a 1 m region (between the horizontal positions of 1.5 m and 2.5 m as seen in Fig. 1) for 4 hours duration. Following that, the entire surface was returned to pre-infiltration conditions (water saturation equal to 0.3).

Synthetic Observations

Hydrological and geophysical measurements were simulated during the ponding experiment and were, thereafter, considered to be the measured data. For this purpose, two boreholes were "placed" in the left and right sides of the model (at x = 1 m and 3 m, respectively, in Fig. 1) extending from the surface to the water table. Permeability measurements were taken from each borehole at 30 cm spacing (corresponding to the same support volume used for the flow modeling) giving 20 point measurements. In each borehole, water saturation measurements were also taken at 20 depths (between -0.1 m and -2.1 m, with a 10 cm interval) at 35 points in time over a period of 12 hours. Zero-mean noise from a normal distribution with variance of 0.01 was added to the synthetic saturation data to simulate measurement error.

In addition, we wish to evaluate the potential benefit of including crosshole GPR measurements in the flow inversion. In particular, zero-offset profile (ZOP) measurements are considered in this study. To obtain a ZOP data set, the source and receiver antennas are placed in separate boreholes and kept at equal depths, and electromagnetic (EM) waves are propagated between the boreholes at different depths, and waveforms are recorded. The travel times may then be used as observational data for inversion. Or, since the travel path is known, the travel times may be converted to EM wave velocity, which can be converted to dielectric constant, and then to water saturation through a petrophysical model (e.g., Roth et al., 1990). A water saturation profile derived from ZOP GPR measurements represents the average inter-borehole saturation for various depths at a given time.

For the present study, horizontally averaged water saturation values are calculated within iTOUGH2 for each time as a proxy for simulated ZOP GPR measurements. This is partly justified by considering that water saturation profiles derived from simulations with a finite difference method matched the pseudo-GPR profile calculated in iTOUGH2 (not shown). Zero-mean noise from a normal distribution with variance of 0.01 was also added to the pseudo-GPR measurements to simulate measurement error.

Inversion with Different Data Types

The inversion procedure is now evaluated for several combinations of data types and compared to models obtained through conditional simulation. Fig. 2b shows a log permeability model generated conditional to some permeability point measurements (at locations indicated with black dots). The model obtained through inversion of the GPR measurements alone is shown in Fig. 2c. Fig. 2d shows the model obtained through inversion using GPR and borehole saturation measurements. For the cases where inversion was performed, (c) and (d), the pilot point locations are indicated by open circles, and the observational measurement locations are marked with open squares (GPR measurements measure the

average water saturation between the two open squares at each depth).

Note that the measured permeability values from (a) are preserved in each of the models shown in (b) – (d). Also note that while the same seed number was used for obtaining these models, a different seed number was used for generating the true model (a).

The permeability model obtained with borehole saturation and GPR measurements (d) appears to best reproduce the true model (a) in the region between the boreholes. For example, both models show a high permeability zone at horizontal position of 1.5m and a depth of -0.7m. However, deviation from the true model is seen between the true model and all other models in the region below -2m (between the boreholes), where no observation data were collected.

How well the models in (b) – (d) predict the observational data (water saturation in the left and right boreholes, and that derived from the pseudo-GPR measurements) is shown in Fig. 3. For the first case, none of the observational data were used to obtain the model, and the mismatch between measured and predicted is large (Fig. 3a). For the second case mentioned above, the GPR measurements alone were used in the inversion, and the measured GPR values are predicted, though the measured borehole saturation values are not (Fig. 3b). For the third case, both data types were used in the inversion, and the values in each synthetic data set are well predicted (Fig. 3c).

Inversion Performance

Performance of the inversion procedure is now evaluated by comparing the real breakthrough curves at several control planes (depicted in Fig. 1) with the breakthrough curves generated using the various models. Several additional cases are included which were not described above: an unconditional simulation, and an inversion using borehole saturation measurements only. Fig. 4 shows that both unconditionally and conditionally simulated models fail to consistently predict breakthrough at each of the control planes. Inversion with borehole saturation values improves the prediction, but not as much as adding GPR measurements. Adding either GPR or both GPR and borehole saturation measurements gives similarly good predictions. Note that for the best cases, predictions at the lowest control plane (CP 3, as labeled in Fig. 1) are less accurate than for the upper two control planes.

When considering lateral variation within the breakthrough curves, slightly different conclusions are drawn regarding the benefit of GPR measurements. While conditional simulations are still highly inaccurate in this case (Fig. 5a), using GPR measurements alone is significantly less accurate than using both GPR and borehole saturation measurements together (compare Fig. 5b and Fig. 5c).

CONCLUSIONS

Inversion with synthetic data indicates that different measurement types, including transient hydrological and geophysical, namely GPR, allow for good prediction of flow phenomena. Pseudo-GPR measurements alone were seen to accurately predict total breakthrough at several control planes. However, to predict lateral variations in breakthrough at the control planes, the combination of GPR measurements with borehole water saturation values were found to work best.

Prediction at the lowest control plane was poorest. This is because improvements to initial realizations are limited in regions without pilot points or observational measurements, like in the region below -2 m depth.

Future work includes the investigation of various GPR measurement configurations (other than ZOP), antenna frequencies (which determine the averaging volume for water saturation estimates) and temporal sampling strategies (i.e., how often GPR surveys are collected). These issues will be more accurately investigated when GPR finite difference modeling is implemented in iTOUGH2.

ACKNOWLEDGMENT

This work was partly supported by (Yoram's funding) and by the U.S. Dept. of Energy under Contract No. DE-AC03-76SF00098.

REFERENCES

Binley, A., Cassiani, G., Middleton, R., Winship, P., Vadose zone flow model parameterization using cross-borehole radar and resistivity imaging, *J. of Hydrology*, 267, 147-159, 2002.

Carrera, J., and S. P. Neuman, Estimation of aquifer parameters under transient and steady state conditions, 2, Uniqueness, stability, and solution algorithms, *Water Resour. Res.*, 22, 211-227, 1986.

Cooley, R. L., An analysis of the pilot point methodology for automated calibration of an ensemble of conditionally simulated transmissivity fields, *Water Resour. Res.,* 36(4), 1159-1164, 2000.

Certes, C., and G. de Marsily, Application of the pilot point method to the identification of aquifer transmissivities, *Adv. Water Resour.*, 14(5), 284-300, 1991.

Deutsch, C.V., and A.G. Journel, GSLIB: Geostatistical Software Library and User's Guide, Oxford Univ. Press, New York, 1992.

Finsterle, S., iTOUGH2 User's Guide. Report LBNL-40040. Lawrence Berkeley National Laboratory, Berkeley, CA, 1999.

Gomez-Hernandez, J. J., A. Sahuquillo, J. E. Capilla, Stochastic simulation of transmissivity fields conditional to both tranmissivity and piezometric data—1. Theory, Journal of Hydrology, 203, 162-174, 1997.

Hubbard, S.S., Rubin, Y. and Majer, E., 1997, Ground-penetrating-radar-assisted saturation and permeability estimation in bimodal systems: *Water Resour. Res.*, 33(5), p. 971-990.

Hollenbeck, K. J., and K. H. Jensen, Maximum-likelihood estimation of unsaturated hydraulic parameters, *J. of Hydrology*, 210, 192-205, 1998.

Kool, J. B., J. C. Parker, M. T. van Genuchten, Determining soil hydraulic properties from one-step outflow experiments by parameter estimation, I, Theory and numerical studies, *Soil Sci. Soc. Am. J.*, 49, 1348-1354, 1985.

de Marsily, G., Spatial variability of properties in porous media: A stochastic approach, in Fundamentals of Transport in Porous Media, edited by J. Bear and M. Y. Corapcioglu, pp. 719-769, Martinus Nijhoff, Boston, 1984.

McLaughlin, D., and L. R. Townley, A reassessment of the groundwater inverse problem, *Water Resour. Res.*, 32(5), 1996.

Mishra, S., and J. C. Parker, Parameter estimation for coupled unsaturated flow and transport, *Water Resour. Res.*, 25(3), 385-396, 1989.

Nelder, J. A., and R. Mead, A simplex method for function minimization, *Comput. Journal*, 7, 308-313, 1965.

Pan, L., and L. Wu, A hybrid global optimization method for inverse estimation of hydraulic parameters: Annealing-simplex method, *Water Resour. Res.*, 34(9), 2261-2269, 1998.

Press, W. H., S. A. Teukolsky, W. T. Vetterling, and B. P. Flannery, Numerical Recipes in Fortran, 2nd. ed., Cambridge Univ. Press, New York, 1992.

Pruess, K., C. Oldenburg, and G. Moridis, *TOUGH2 User's Guide, Version 2.0*, Report LBNL-43134, Lawrence Berkeley National Laboratory, Berkeley, Calif., 1999.

Roth, K.R., R. Schulin, H. Fluhler, and W. Attinger, Calibration of time domain reflectometry for water content measurement using a composite dielectric approach, *Water Resour. Res.*, 26, 2267-2273, 1990.

Russo, D., E. Bresler, U. Shani, and J. C. Parker, Analyses of Infiltration Events in Relation to Determining Soil Hydraulic Properties by Inverse Problem Methodology, *Water Resour. Res.*, 27(6), 1361-1373, 1991.

Simunek, J., and M.T. van Genuchten, Estimating soil hydraulic properties from tension disc infiltrometer data by numerical inversion, *Water Resour. Res.*, 32(9), 2683-2696, 1996.

van Genuchten, M. Th., 1980, A closed-form equation for predicting the hydraulic conductivity of unsaturated soils: *Soil. Sci. Soc. Am. J.*, 44, p. 892-898.

Wen, X. -H., C. V. Deutsch, and A. S. Cullick, Construction of geostatistical aquifer models integrating dynamic flow and tracer data using inverse technique, *J. of Hydrology*, 255, 151-168, 2002.

Yeh, T.-C., S. Liu, R. J. Glass, K. Baker, J. R. Brainard, D. Alumbaugh, and D. LaBrecque, A geostatistically based inverse model for electrical resistivity surveys and its applications to vadose zone hydrology, *Water Resour. Res.*, 38(12), 1278, 2002.

Zhou, Z.-Y., M. H. Young, Z. Li, and P. J. Wierenga, Estimation of depth averaged unsaturated soil hydraulic properties from infiltration experiments, *J. of Hydrology*, 242, 26-42, 2001.

Zijlstra, J., and J. H. Dane, Identification of hydraulic parameters in layered soils based on a quasi-Newton method, *J. of Hydrology*, 181, 233-250, 1996.

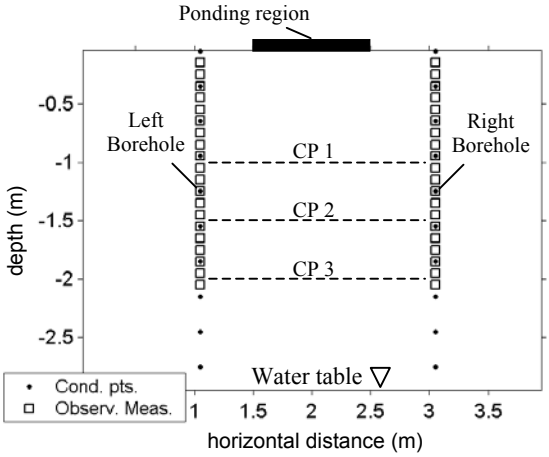

Figure 1. Vadose zone model used in numerical example. Boreholes are located at horizontal positions of 1 m and 3 m. Permeability measurements are taken from each borehole at 30 cm spacing (shown as black dots), water saturation measurements are taken in the boreholes (at open squares), and the pseudo-GPR measurements represent horizontally averaged water saturation values between the boreholes (between open squares). Control planes used to test inversion performance are denoted by CP 1, CP 2, and CP 3.

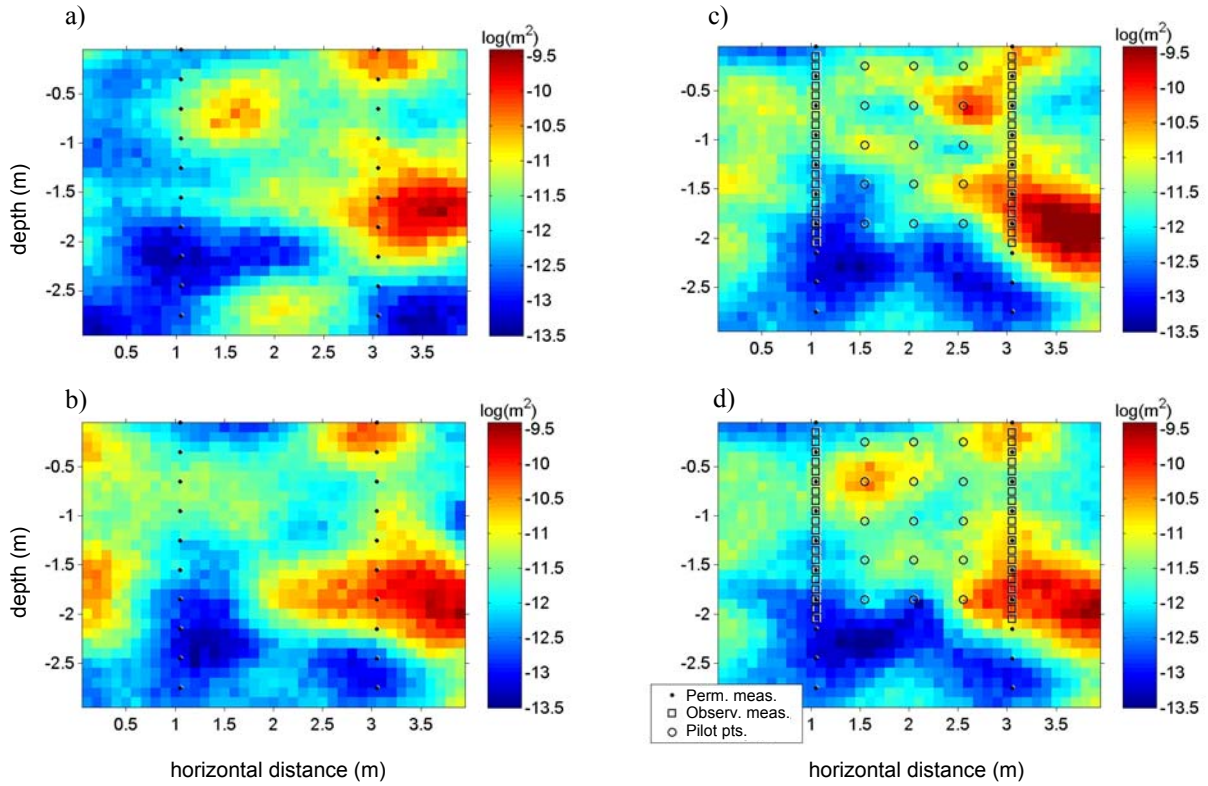

Figure 2. True log permeability model: a) used to generate synthetic observations during a ponding experiment, b) obtained through conditional simulation, c) obtained through inversion using GPR measurements, and d) obtained through inversion using GPR and borehole saturation measurements. The ponding region is indicated in Fig. 1.

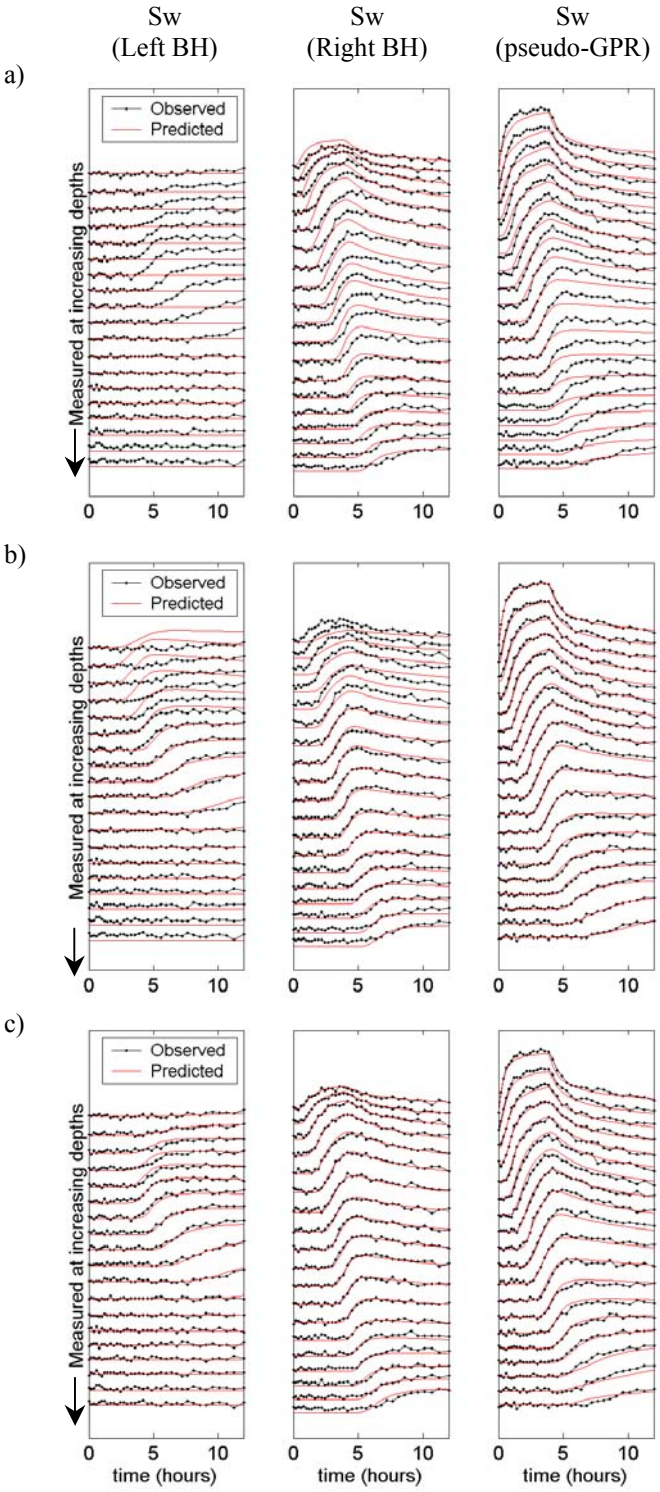

Figure 3. Misfit between simulated (shown with black dots) and predicted (shown with red lines) water saturation in left borehole (1st column), right borehole (2nd column), and horizontally averaged water saturation from pseudo-GPR measurements (3rd column) for one realization. Three cases are shown: a) conditional simulation, b) inversion using GPR measurements and c) inversion using GPR and borehole saturation measurements.

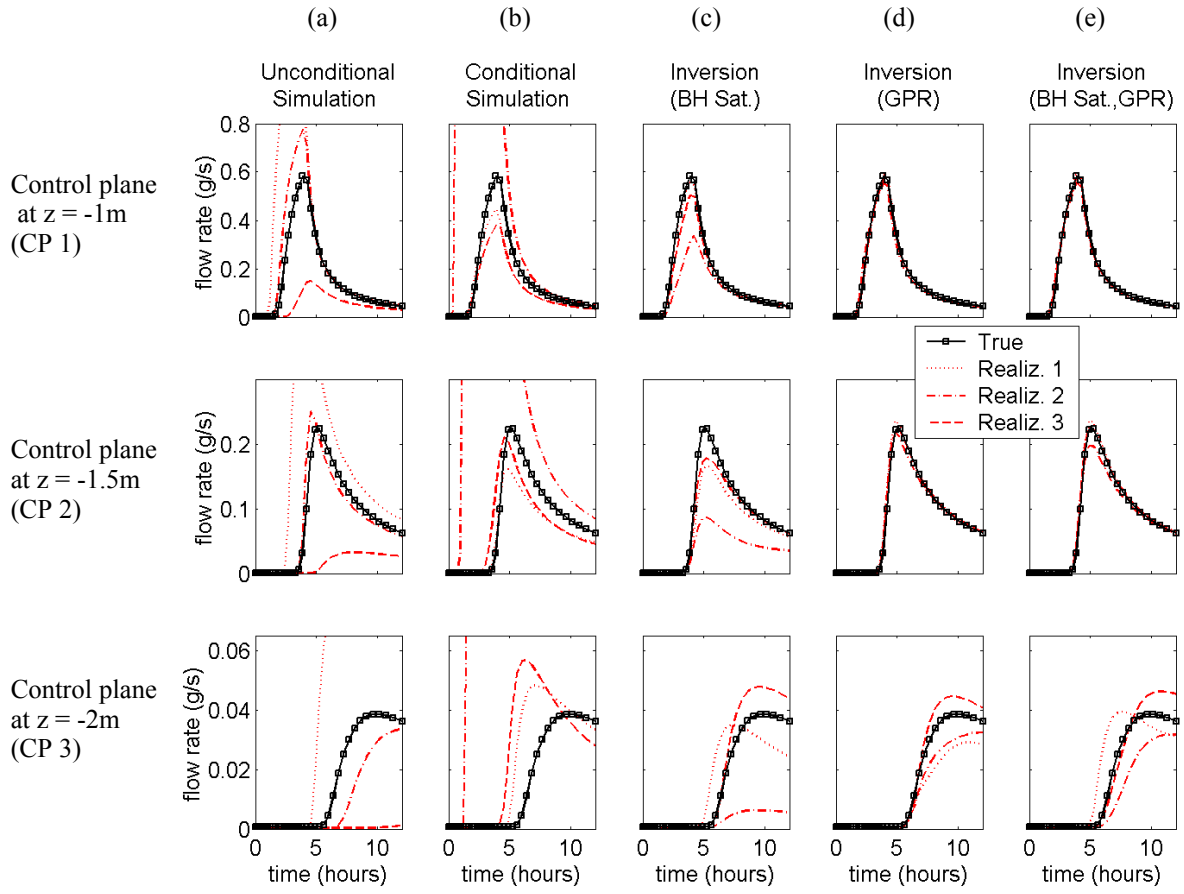

Figure 4. Breakthrough curves (total flow rates) at three control planes CP 1, CP 2, and CP 3 (defined in Fig. 1) for these cases: unconditional simulation (column a), conditional simulation (column b), inversion with left and right borehole saturation values (column c), inversion with only GPR (column d), and inversion with GPR along with left and right borehole saturation values (column e). Breakthrough for the true model is shown with black squares, and inversions using three different seed numbers (representing three realizations) are shown in red.

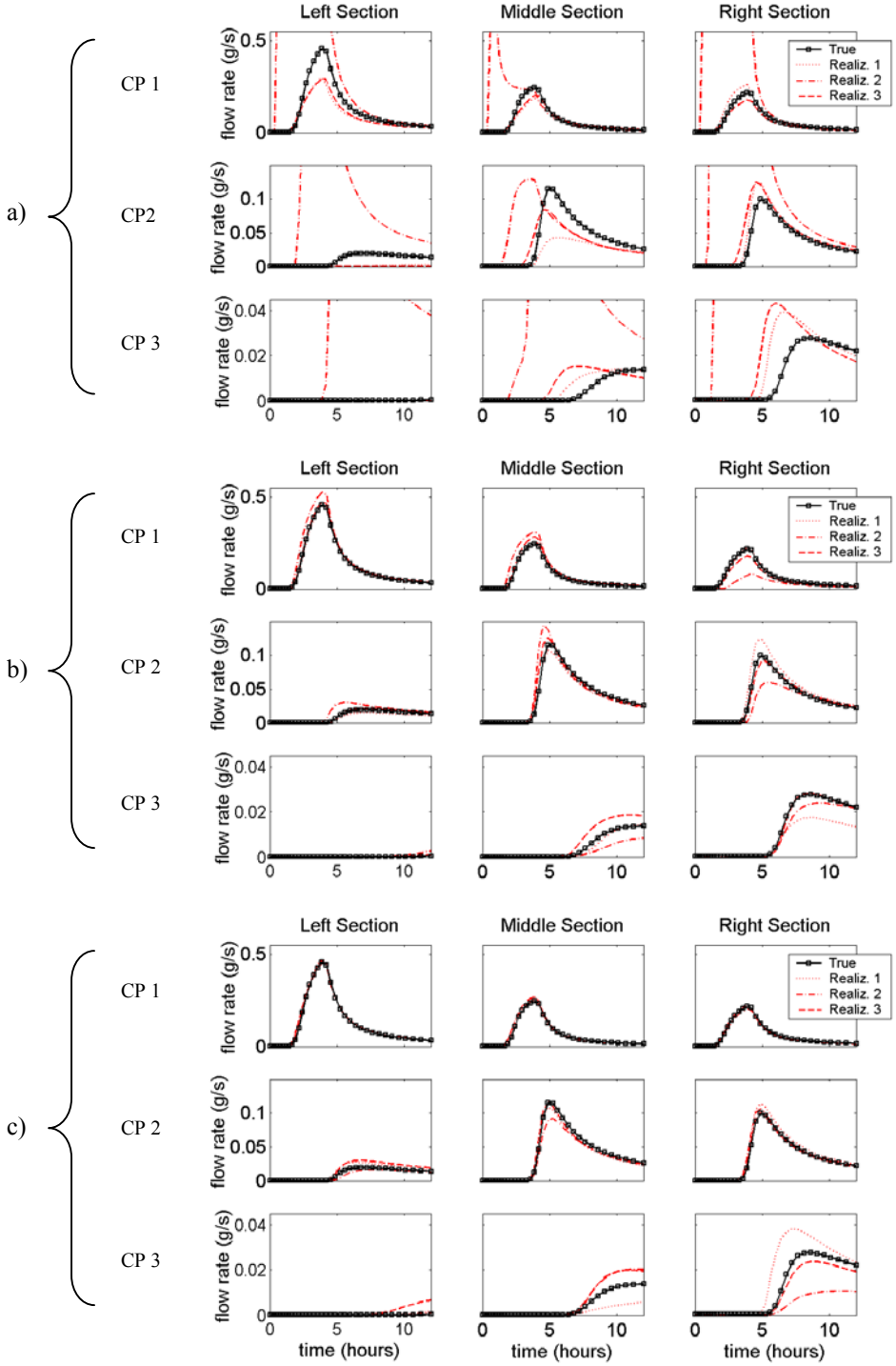

Figure 5. Breakthrough curves (total flow rates) for three sections of each control planes CP 1, CP 2, and CP 3 (defined in Fig. 1). Flow rate of each control plane is shown, divided into the left side (1st column), middle (2nd column), and right side (3rd column). Three cases are shown: a) conditional simulation, b) inversion using GPR measurements and c) inversion using GPR and borehole saturation measurements. Breakthrough for the true model is shown with black squares, and inversions using three different seed numbers (representing three realizations) are shown in red.